buildings

MDPI

Article

RETRACTED: Mechanical, Durability, and Microstructural Evaluation of Coal Ash Incorporated Recycled Aggregate Concrete: An Application of Waste Effluents for Sustainable Construction

Ali Raza [1,*], Noha Saad [2], Khaled Mohamed Elhadi [3], Marc Azab [2,*], Ahmed Farouk Deifalla [4], Ahmed Babeker Elhag [3] and Khawar Ali [1]

[1] Department of Civil Engineering, University of Engineering and Technology, Taxila 47050, Pakistan
[2] College of Engineering and Technology, American University of the Middle East, Egaila 54200, Kuwait
[3] Department of Civil Engineering, College of Engineering, King Khalid University, P.O. Box 394, Abha 61411, Saudi Arabia
[4] Structural Engineering Department, Faculty of Engineering and Technology, Future University in Egypt, New Cairo 11845, Egypt
* Correspondence: ali.raza@uettaxila.edu.pk (A.R.); marc.azab@aum.edu.kw (M.A.)

check for updates

Citation: Raza, A.; Saad, N.; Elhadi, K.M.; Azab, M.; Deifalla, A.F.; Elhag, A.B.; Ali, K. RETRACTED: Mechanical, Durability, and Microstructural Evaluation of Coal Ash Incorporated Recycled Aggregate Concrete: An Application of Waste Effluents for Sustainable Construction. *Buildings* **2022**, *12*, 1715. https://doi.org/10.3390/buildings12101715

Academic Editors: Zhihai He, Kunjie Fan, Dong Zhang and Nanting Yu

Received: 28 September 2022
Accepted: 14 October 2022
Published: 17 October 2022
Retracted: 16 June 2025

Publisher's Note: MDPI stays neutral with regard to jurisdictional claims in published maps and institutional affiliations.

Copyright: © 2022 by the authors. Licensee MDPI, Basel, Switzerland. This article is an open access article distributed under the terms and conditions of the Creative Commons Attribution (CC BY) license (https://creativecommons.org/licenses/by/4.0/).

Abstract: This study has endeavored to produce eco-friendly coal ash-incorporated recycled aggregate concrete (FRAC) by utilizing wastewater effluents for environmental sustainability. The mechanical and durability efficiency of the FRAC manufactured were explored using different kinds of effluent by performing a series of tests at various ages. The considered kinds of effluent for the mixing of FRAC were collected from a service station, as well as fertilizer, textile, leather, and sugar factories. Scanning electron microscopy (SEM) was utilized to judge the microstructural behavior of the constructed concrete compositions. The outcomes revealed that using textile factory effluent in the manufacturing of FRAC depicted peak compressive and split tensile strength improvements of 24% and 16% compared to that of the FRAC manufactured using potable water. The application of leather factory effluent for the manufacturing of FRAC portrayed the highest water absorption (13% better than the control mix). The application of fertilizer effluent in the manufacture of FRAC presented the greatest mass loss (19% enhanced than the control mix) due to H_2SO_4 solution intrusion and the ultimate chloride ion migration (16 mm at twenty-eight days of testing). The summation of coal ash improved the mechanical behavior of the concrete and also caused a reduction in its durability loss of. The SEM analysis depicted that the textile factory effluent presented the most densified microstructure with the development of ettringite needles and CSH gel having refined the ITZ.

Keywords: coal ash; recycled aggregate concrete; waste effluent; compressive strength; acid attack resistance

1. Introduction

A significant quantity of construction and demolition waste (CDW) material collected from the removal of outdated infrastructures must be effectively utilized for sustainable development and the environment. By satisfying the desire for natural resource preservation and environmentally friendly, low-carbon, and sustainable building, recycled aggregate concrete (RAC) helps in the reduction of landfill space necessary for CDW and aggregates transportation charges [1–6]. Furthermore, CO_2 emissions are rising due to increased cement production, which accounts for more than 5% of overall global CO_2 release [7]. The consequences of cement production can be minimized by replacing them with cementitious materials such as coal ash, which can efficiently diminish the footprint of cement [8,9]. In summation, rivers and landfills receive a substantial amount of runoff and effluents. When humans or animals come into contact with effluent or its products, they can be exposed to

RETRACTED

This paper has been retracted. A retraction notice was published on 16 June 2025 in *Buildings* **2025**, *15*, 2064. https://doi.org/10.3390/buildings15122064

harmful microorganisms that can cause illnesses such as cryptosporidiosis (severe stomach cramps, diarrhea, or vomiting) and gastroenteritis giardiasis [10]. Moreover, due to severe environmental regulation and the refusal of landfill sites to be built near communities, there is an increasing demand for alternative waste management solutions [11]. The production of concrete involves one trillion gallons of water each year [12]. As a result, to maintain an equilibrium between the demand and supply of fresh water, freshwater use must be limited, notably in the construction industry and other industries [13,14]. Concrete might be manufactured without being treated, saving money on effluent treatment and avoiding negative environmental and biological effects [14,15].

Many studies have been executed to investigate the freshness, mechanical, and durability aspects of RAC produced using fresh water, with the conclusion that RAC performs poorly when compared to conventional concrete [5,16–21]. The literature shows that the inclusion of fly ash to the RAC with glass fibers and recycled coarse aggregates increased the later-age mechanical properties and decreased the loss in durability caused by the summation of both glass fibers and recycled coarse aggregates (RCA) [9,22–24]. Previous literature shows that the substitution of natural coarse aggregate (NCA) with RCA reduces the compressive strength (CS) of concrete by 10–20% [25–28]. The CS of RAC was abridged by 20–25% by completely replacing the NCA with RCA when other ingredients of the concrete were kept constant for both RAC and natural aggregate concrete [29]. Obtaining RCA from a single source is a good way to enhance the CS of RAC. RCA collected from different resources has variable properties which affect the CS of RCA more significantly [29–34]. The CS of RAC is also influenced by the mortar bonded to coarse aggregates. The CS of RAC was reduced by 10% as a result of the 34% bonded paste for aggregate sizes of 10–20 mm [33].

Several studies show that various types of effluent can be utilized to make concrete. No influence on setting time was observed when processed household effluent was utilized rather than potable water [35]. Furthermore, the concrete's CS increased by 1.5% when concrete was soaked with treated effluent. The use of household sewage instead of potable water did not affect the setting time [36]. Production of concrete with waste wash water coming from ready-mixed concrete plants had 96% more strength than concrete made with freshwater [37]. Treated effluent enhanced the setting time and CS of concrete equated with potable water [38,39]. For the first 180 days, concrete made with primary and secondary biologically treated waste increased CS by 17%. Meanwhile, axial strength in secondary processed effluent was reduced by nearly 18% when compared to primarily treated waste. Furthermore, concrete made with secondary treated effluent had an improved water absorption rate (WA) [40].

Some of the previous studies show that the application of concrete wash water for the mixing process significantly improves the mechanical properties of concrete [41,42]. As per test results, concrete built with a mix of potable water had an improved CS over concrete made with micro-silica [43]. When Wasserman [44] examined the CS of concrete, the author discovered that concrete made using concrete wash water had more improved CS than concrete made with drinkable water. Researchers discovered that when steel slag and effluent were added to bio-concrete, the drop in bio-concrete efficiency could be offset by using bacterially manufactured calcium carbonate [45,46]. The WA of bio-concrete was lowered, while the tensile and CS increased by 12.5% and 31%, correspondingly. The loss of weight is a major concern that occurs when the pH level of water fluctuates. The degradation of concrete accelerates as the pH level of the water is reduced [47–49].

After carrying out a detailed literature review, it can be established that the incorporation of RCA, coal ash, and waste effluent into the concrete manufacturing process can help in building a more sustainable construction. Furthermore, this research area needs in-depth analysis to check the combined applicability of coal ash, RCA, and wastewater effluents for the production of concrete, because no study has considered their utilization at the same time. It is necessary to assess the mechanical and durability properties of coal ash-integrated recycled aggregate concrete (FRAC) with numerous types of effluent for

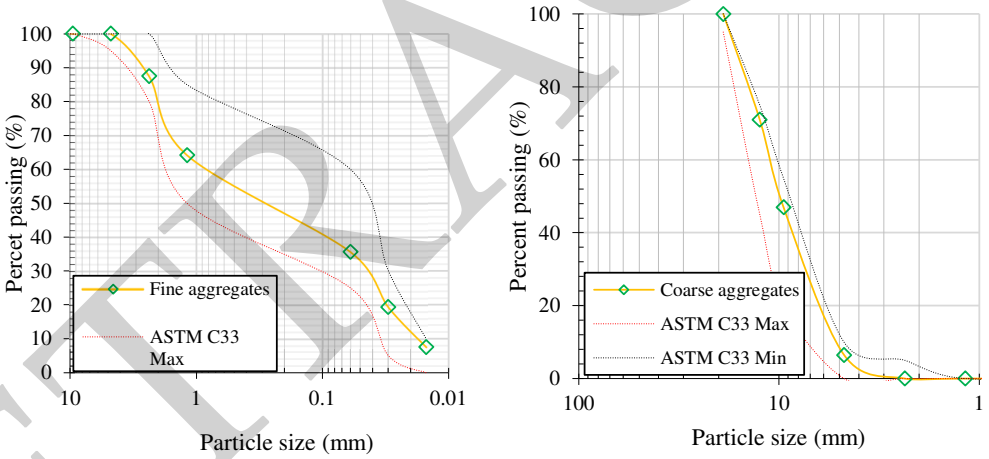
RETRACTED

their practical applications leading toward sustainable construction. The purpose of this study is to investigate the CS, split tensile strength (STS), water absorption, chloride ion migration, and resistance to the sulfuric acid attack of FRAC at different testing ages due to the use of different effluents like leather (LED), fertilizer (FER), textile (TEX), sugar (SUG), and service station (SER) effluents. Scanning electron microscopy (SEM) analysis examined the microstructural properties of fabricated concrete compositions. The behavior of concrete made with effluent and concrete cast with potable water was compared. In summation, a statistical analysis was executed to establish the importance of variability in several FRAC mix parameters. This study proposes sustainable concrete for development works.

2. Experimental Program

2.1. Materials and Properties

A grade 42R Portland Cement was used as a cementitious material in accordance with ASTM C150/C150M [50]. Table 1 lists the fundamental mechanical properties and chemical composition of cement. The plain concrete cylinders comprising CS of 30 to 45 MPa were crushed to produce the RCA. The RCA was 12 mm in size at maximum. Readily accessible local sand satisfied the criteria of ASTM C33 [51] utilized in this research. Table 2 lists the qualities and properties of RCA and sand. Figure 1 depicts their sieve analysis curves. The coal ash was produced by DIRK Pozzoplast and has its specifications listed in Table 3. A SEM image of coal ash is presented in Figure 2. Six different types of effluent were collected from their respective sources to be utilized in the manufacturing of FRAC. Each type of effluent completely replaced potable water. The composition of all forms of effluents utilized in this study is listed in Table 4.



(**a**) (**b**)

Figure 1. Sieve analysis of aggregates (**a**) sand (**b**) RCA.

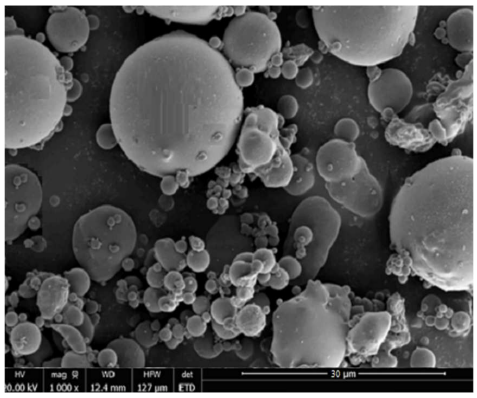


Figure 2. SEM analysis of coal ash particles.

RETRACTED

Table 1. Parameters of Portland cement.

Physical Properties		Chemical Properties	
Parameter	**Value**	**Compound**	**Percentage**
Consistency [52]	28.90%	SiO_2	19.2%
Fineness (Blaine Test)	2765 (cm^2/g)	CaO	58.1%
Specific surface area [53]	325 m^2/kg	Fe_2O_3	6.0%
Soundness [54]	No expansion	Na_2O	0.4%
Specific gravity [55]	3.0	Al_2O_3	5.7%
Initial setting time [56]	110 min	SO_3	2.2%
Final setting time [56]	225 min	MgO	5.3%
Strength at 3 days [57]	38.2 MPa	Loss of ignition	2.9%
Strength at twenty-eight days [57]	42.5 MPa	K_2O	0.8%

Table 2. Characteristics of RCA and sand.

Property	Sand	RCA
Water absorption after 24 h (%)	2.33	7.30
Dry density (kg/m^3)	1630	1295
Specific gravity	2.62	2.23
Fineness modulus	2.43	-
Maximum size (mm)	4.75	12.0
Minimum size (mm)	-	4.75

Table 3. Composition of coal ash.

Chemical Properties		Physical Properties	
Compound	**Percentage**	**Parameter**	**Value**
SiO_2	57.9%	Consistency [52]	25.98%
CaO	3.21%	Specific surface area [53]	389 m^2/kg
Fe_2O_3	2.3%	Fineness (Blaine Test)	2950 (cm^2/g)
Na_2O	1.02%	Soundness [54]	No expansion
Al_2O_3	31.32%	-	-
SO_3	1.01%	-	-
MgO	0.7%	-	-

Table 4. Characteristics of all kinds of effluent studied in this research.

Parameter (Unit)	POT	LED	FER	TEX	SUG	SER
pH value	7.00	7.30	2.50	7.10	7.20	6.00
Hardness (mg/L)	357.7	706.58	2508.8	335.16	2077.6	362.6
Alkalinity (mg/L)	80.36	95.06	0.50	47.04	120.54	84.28
Bicarbonates (mg/L)	33.56	37.88	0.40	296	135	43
DO (mg/L)	6.17	2.74	2.35	5.19	2.94	2.54
COD (mg/L)	18.22	412.58	1024.1	117.6	931	191.6
BOD (mg/L)	14.70	304.78	597.8	68.6	705.6	127.6
TSS (mg/L)	33.32	491.96	64.68	25.48	71.54	66.64
TDS (mg/L)	880.04	1074.08	5117.56	380.24	4018.98	480.2
Turbidity (NTU)	1.07	245	3.18	1.20	24.5	36.26
Conductivity (m-s/cm)	1.37	1.82	8.33	0.98	6.46	0.86
Fluoride (mg/L)	0.39	1.12	0.09	1.69	0.42	0.11
Chloride (mg/L)	14.7	333.2	858.48	62.13	844.76	245
Sulphate (mg/L)	8.82	739.9	927.08	102.9	205.8	113.68
Iron (mg/L)	0.76	0.85	3.52	0.94	1.45	1.20
Zinc (mg/L)	-	1.32	-	-	0.18	-
Nitrate (mg/L)	1.86	137.2	70.56	2.54	37.24	11.76

RETRACTED

2.2. Testing Methodology

The RCA was soaked for 10 min to achieve saturation as a pre-treatment [58]. The six FRAC compositions developed with various types of sewage were a potable water mix (POT), leather factory effluent mix (LED), fertilizer factory effluent mix (FER), textile factory effluent mix (TEX), sugar factory effluent mix (SUG), and service station effluent mix (SER). The FRAC mix developed with a potable water mix (POT) was used as the control mix for comparison purposes. The control mix also contained coal ash and recycled aggregates like the other mixes, but its mixing was performed using potable water instead of wastewater. Every type of effluent was utilized in equal amounts in all of the FRAC blends. In all of the representatives, coal ash was utilized as a 20% substitute for cement as utilized in a previous study [22]. Eighteen different cylindrical representatives were cast for the determination of the CS and STS at all ages (7, 28, and 90 days) from each of these FRAC mixtures. An average of three representatives was used to discuss the results at various testing ages of each mix. A compression testing machine with a loading capacity of 2000 kN was utilized for assessing the CS and STS of fabricated samples. The dimensions of the representatives are 150 mm × 300 mm. Thirty-six representatives with dimensions of 50 mm × 100 mm were collected to investigate the WA. Thirty-six representatives sized at 100 mm × 100 mm (height × diameter) were also made to investigate chloride ion penetration. Fifty-four cube representatives sized at 100 mm × 100 mm were also made to study sulfate attack resistance. The materials and quantities utilized for each type of FRAC mix are listed in Table 5.

Table 5. Quantities of different components in the FRAC (kg/m^3).

Cement	RCA	Fine Aggregates	Water Content	Coal Ash	w/c Ratio
331	1155	625	166	83	0.5

A mixer was utilized for 10 min at a rotating speed of 20 rpm with a volumetric capacity of 0.15 m^3. The aggregates were first mixed with half the quantity of the water, then the remaining water, cement, and coal ash were added and stirred for 5 min to obtain a homogeneous FRAC mix. Slump tests were executed under ASTM/C143 [59]. All effluent groups have slump values in the range of 85 to 110 mm. All of the FRAC blends were cured with ordinary water. CS and STS were two separate mechanical characteristics identified for every FRAC mix at varying ages. The representatives were tested for CS using ASTM C39 [60] and for STS using ASTM C496 [61] at seven, twenty-eight, and ninety days. Chloride ion migration, WA, and acid attack were the durability parameters evaluated for the six different kinds of FRAC mixture. The WA property was tested, agreeing with ASTM C1585 [62]. The representatives were cured for twenty-eight days in room temperature water to assess their resistance to H_2SO_4. The representative was soaked in 4% H_2SO_4 for an acid attack after drying for 24 h at 50 °C.

The representatives were further cured in normal water for twenty-eight and ninety days before being oven-dried for 24 h at 50 °C to find chloride ion absorption. The representatives were then allowed to cool to room temperature before being soaked in a 4% NaCl solution for 56 days. The representatives were then split, agreeing with ASTM C496 [61], and sprinkled with a 1N $AgNO_3$ solution in water. The $AgNO_3$ started a reaction with the chloride ions and AgCl was obtained as a product. A silver-colored compound was utilized to assess chloride ion mobility in concrete made with various types of effluent. Previous attempts led to the development of this working method [22,63]. SEM analysis of fractured representatives was executed. Before performing the tests, the fractured surface of each representative was cleaned and covered with gold to avoid the production of charge.

RETRACTED

3. Discussion of Results

3.1. Mechanical Performance

3.1.1. Compressive Strength

The CS of FRAC combinations is visualized in Figure 3. The TEX mix had the highest CS across all testing ages, while the LED FRAC mix had the lowest CS. A control mix (POT) was cast to compare the outcomes of FRAC compositions cast with different types of effluent. POT determined CS to be 14.9 MPa at a curing duration of seven days. The CS at twenty-eight days had increased by 28.5%, resulting in a value of 21 MPa. The CS had risen to 25.6 MPa after ninety days, which was 140 percent improved over the CS measured after seven days. As a result, the CS of the POT mix gradually increased as the testing age progressed.

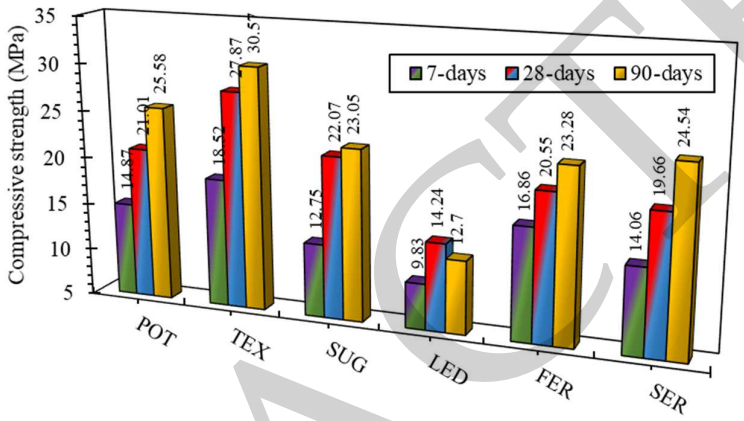


Figure 3. CS of FRAC compositions at seven, twenty-eight, and ninety days.

The CS of the TEX mix improved significantly compared to that of the POT mix. The TEX blend had a CS of 18.5 MPa for a seven-day curing time, which improved 19% more than the POT on average. The TEX blend had a CS of 27.8 MPa after twenty-eight days, which was 24% more improved than the POT. The FER blend indicated an enhanced strength of 30.5 MPa. Its mean strength was 15% improved over the strength indicated by the POT after a curing period of ninety days. The CS obtained when TEX was utilized to manufacture FRAC blends was more improved than the POT. The fluoride and bicarbonates in the TEX were combined with the Al_2O_3 in OPC and coal ash to generate calcium fluoroaluminate that resulted in an improved CS by setting the cement and increasing the speed of hydration, as this mineral is extremely reactive [45,64,65]. Coal ash has been shown to benefit the CS of FRAC because of the pozzolanic action of CH and coal ash. In concrete, coal ash works as a filler between the cement and sand, generating a CSH gel that improves binding strength. The CS of the FRAC mix was more improved than that of the POT mix after seven days of curing but decreased at twenty-eight and ninety days. The FER mix had a CS of 16.8 MPa, which was 11.5 percent more improved than the POT's strength during the seven-day curing period. The FER mix had a 2.1 percent decrease in CS with a value of 20.5 MPa at twenty-eight days of curing. When compared to the POT, the CS in the FER mix decreased by 8.5 percent over ninety days. Despite remaining, a 12.5 percent improvement over the CS was reported at twenty-eight days. The increasing quantities of BOD and COD in FER result in a decrease in the CS of the FER mix at the ages of twenty-eight and ninety days [66].

The CS decreased considerably when LED was utilized to mix the concrete. It had a CS of 9.8 MPa, 14.2 MPa, and 12.7 MPa for seven, twenty-eight, and ninety days, respectively. The CS of the LED had an average CS of 32%, 31%, and 49% lower than the CS demonstrated by the POT FRAC blend on testing days seven, twenty-eight, and ninety, separately. The high content of TSS in LED may be responsible for this reduction in strength. Furthermore, the presence of organic matter in LED water, which was spongy in nature, produced an

RETRACTED

impact on the water demand resulting in reduced mechanical performance of the LED mix [67,68]. The water-to-cement ratio of the LED mix increased when it was being mixed. This was the major reason for the strength reduction. The composition of blended organic waste has a considerable impact on the concrete CS. During the blending process of concrete, these effluents contain water and then secrete it when compacted during casting. The w/c ratio was one of the main reasons for the decline in CS. The drop in CS could potentially be due to the existence of organic contaminants in LED, such as a significant percentage of sulfates of organic origin. In summation, the strength development is directly affected by the performance of the mixing water utilized. Although the LED mix's strength increased to 30.5 percent after twenty-eight days, it showed a decline of 10.5 percent after ninety days of curing time. A large number of organic chemicals in the LED mix react with the cementitious materials over time. As a result, a decline in LED mix strength was observed. The CS of the LED blend dropped due to the high levels of sulfate in the LED after a curing period of ninety days. The other main reason behind the reduction in CS of the LED mix was the high amount of phosphate, which resulted in a delay in the hydration process, leading to a weak ITZ. In particular, cement particles react with phosphate salts and fabricate a coat of Ca phosphate. This coat, sequentially, separates water from cement particles and therefore postpones the hydration process of cement [69]. Furthermore, the hydration of cement in attendance of zinc was also hindered because of the fabrication of an amorphous coat of $Zn(OH)_2$, which then changed into $CaZn_2(OH)_6 \cdot 2H_2O$. The chemical processes explaining the effect of zinc on the hydration of C_3S are shown in the following chemical reactions. Such processes suspend the production of C_3S hydration by-products [70]. Moreover, the availability of TSS in LED-enhanced concrete porosity and deteriorated the ITZ layers and therefore reduced the CS of the concrete. Correspondingly, Arooj et al. [71] concluded that effluent concrete presented reduced by 11% to 15% CS compared to freshwater concrete.

$$Zn^{2+} + 2OH^- \rightarrow Zn(OH)_2$$

$$Zn(OH)_2 + 2OH^- \rightarrow 2H_2O + ZnO_2^{2-}$$

$$2ZnO_2^{2-} + C_3S/O - Ca^{2+} + 6H_2O \rightarrow C_3S/O \rightarrow CaZn_2(OH)_6 \cdot 2H_2O + 2OH^-$$

The CS of the concrete was slightly affected when SER was utilized in the concrete mix. It had a CS of 14 MPa, 19.6 MPa, and 24.5 MPa after curing periods of seven, twenty-eight, and ninety days, respectively. The POT mix produced results that were 5%, 5.5%, and 4.50% lower than the CS indicated by the POT FRAC mix at seven, twenty-eight, and ninety days, separately. All the little variations show that when SER is utilized to mix concrete, the concrete CS has no noticeable influence. The presence of large amounts of BOD and COD may explain why SER demonstrated a loss in strength at all periods of testing [66]. The concrete CS dropped to 13.5% when SUG was utilized after a curing period of seven days, whereas the POT mix increased to 5.5% after twenty-eight days of casting. The concrete showed enhanced strength as a result of the longer time it took for the cement paste to cure and the increased surface area of the cement particles [72,73]. After ninety days, the concrete CS dropped to 9.5% when compared to the POT mix. The presence of C_3S in the cement may cause retardation in the hydration process, which is a major cause of a decrease in CS [74,75]. Figure 4 depicts the comparative CS of all FRAC mixtures after seven, twenty-eight, and ninety days of testing.

RETRACTED

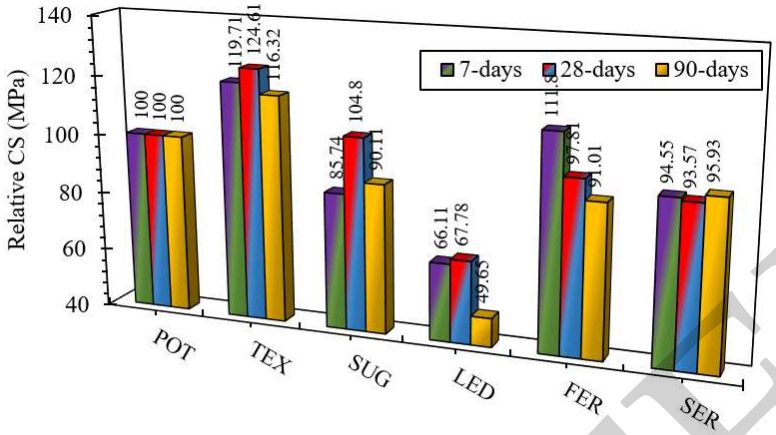


Figure 4. CS of FRAC compositions with regard to POT at seven, twenty-eight, and ninety days of testing.

3.1.2. Split Tensile Strength

The STS produced by FRAC blends prepared with diverse forms of waste are shown in Figure 5. Experimentation was conducted agreeing to ASTM C496 [76] after a curing period of seven, twenty-eight, and ninety days. The average STS of the POT mix was 1.8 MPa, 2 MPa, and 2.4 MPa after seven, twenty-eight, and ninety days. This means that the POT blend had an STS of 115% after ninety days of its strength at twenty-eight days. The highest STS was found in the TEX blend, but the lowest was found in the LED blend. The improvement in particle size was observed due to the summation of coal ash to the concrete matrix by filling the voids, which led to an improvement in the STS of FRAC. It transformed the binder mixture into CSH gel, which created a strong matrix between the FRAC particles. The STS of the TEX blend was 2 MPa, 2.3 MPa, and 2.8 MPa after seven, twenty-eight, and ninety days. These strengths were 12.5%, 16%, and 16.5% more improved than the STS of the POT mix after seven, twenty-eight, and ninety days. The STS of the TEX blend was improved because the TEX had a lower proportion of bicarbonates. This indicates that adding more bicarbonates to concrete diminishes its STS [77].

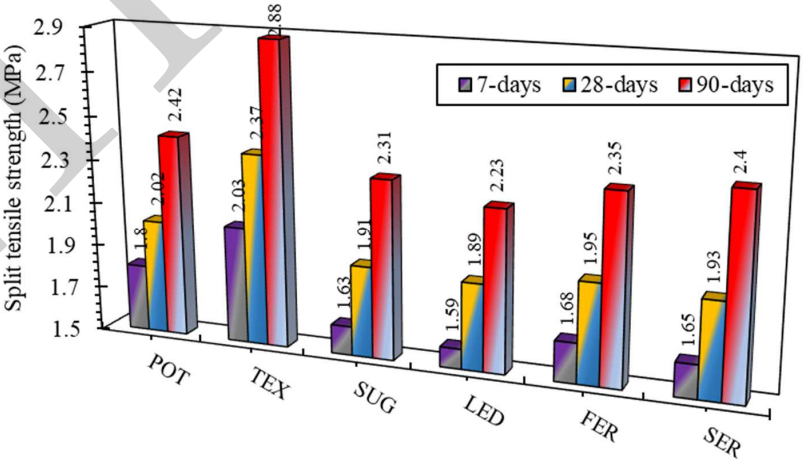


Figure 5. STS of FRAC compositions at seven, twenty-eight, and ninety days of testing.

Agreeing with the FER mix, STS was 1.7 MPa, 1.9 MPa, and 2.3 MPa at seven, twenty-eight, and ninety days. FER in the concrete mix shows a decrease in STS of up to 6.5%, 4.5%, and 4% after seven, twenty-eight, and ninety days. An analysis was conducted on the reduction in STS when several types of effluent were utilized. The STS was calculated with the substitution of LED mix and was reduced by 10.5%, 7%, and 8.5% after seven, twenty-eight, and ninety days relative to the POT mix. In comparison to the POT mix, the

RETRACTED

SER mix had STSs of 93%, 94.5%, and 98.5% after a curing period of seven, twenty-eight, and ninety days. The SUG mix had an STS of 1.6 MPa, 1.9 MPa, and 2.3 MPa after the curing periods of seven, twenty-eight, and ninety days. Several FRAC compositions (i.e., FER, LED, SER, and SUG) showed lower STS, which could be explained by the fact that these effluents are high in BOD, COD, and total suspended particles (TSS) [78]. The STS of concrete drops as the amount of chloride in the concrete surges [79], causing a reduction in the STSs of chloride-rich FRAC compositions. In summation, the pH of these combinations was lower. The decline in STS is related to a lower pH value [80]. Figure 6 illustrates a measure of the relative percentage of STS as seen by multiple FRAC compositions versus the POT mix at various ages.

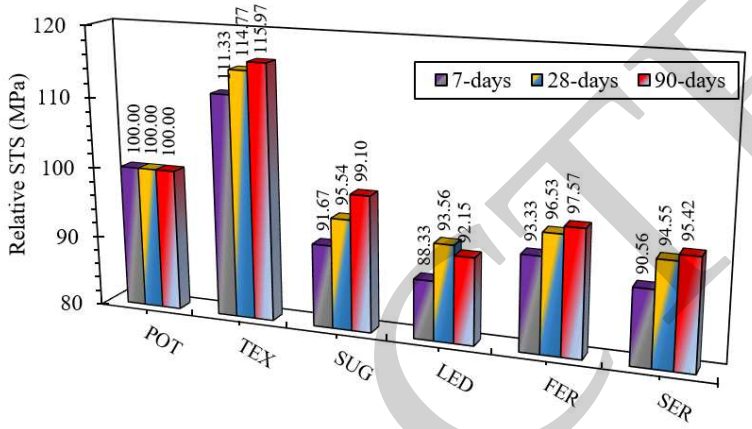


Figure 6. STS of FRAC compositions with regard to POT at seven, twenty-eight, and ninety days of testing.

3.2. Durability Performance

3.2.1. Water Absorption

WA determines how many water-accessible pores there are in concrete. The high level of WA affects the properties of concrete by allowing numerous toxic chemicals to penetrate and react with the cement ingredients, which causes reinforcement corrosion. Figure 7 depicts the WA produced by different FRAC compositions. Almost all of the representatives had an enhanced WA level. This may be because the WA values for RCA (7.30%) and fine aggregates (2.31%) utilized in this investigation were larger. As previously stated, the various types of effluents utilized in concrete production have no discernible effect on the WA of concrete [81].

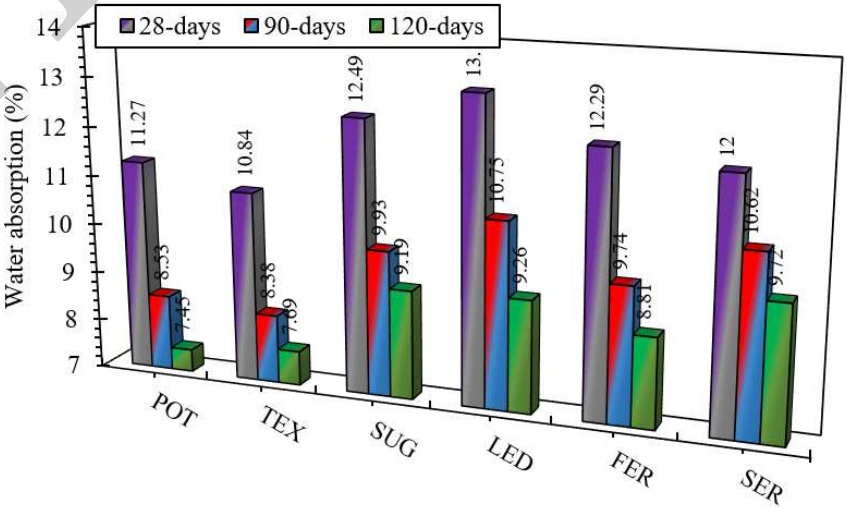


Figure 7. WA of FRAC compositions at twenty-eight, ninety, and one hundred and twenty days of testing.

RETRACTED

FRAC blends showed a decline in the characteristics of WA over time. The POT mix's WA was 11.2 percent, 8.5 percent, and 7.4 percent at twenty-eight, ninety, and one hundred and twenty days, respectively, indicating a decline in WA over time. The WA shown by the TEX blend was less relative to the POT. The WA was 95.5%, 98%, and 97% at twenty-eight, ninety, and one hundred and twenty days, respectively, relative to the POT. This decline in WA could be linked to a reduction in chloride levels in the concrete. The density of concrete decreases as the number of chlorides surges, which results in low STS as well as CS [79]. The inclusion of coal ash reduced the WA of FRAC due to the influence of the filler and the formation of CSH gel after the pozzolanic interaction of coal ash particles and chlorides.

The WA levels of the FER blend were 9%, 12%, and 15% more improved than those of the POT at curing ages of 28, 90, and 120 days, respectively. The LED mix had the highest WA levels of all the representatives, with values of 13.1%, 10.7%, and 9.3% at twenty-eight, ninety, and one hundred and twenty days, respectively, which were 13.5%, 21%, and 19.5% more than the POT mix. The significant volume of organic effluent in LED created a substantial number of pores, which resulted in a surge in WA. These effluents absorb the water during the blending process and eject it during the pouring phase, resulting in an improved w/c ratio and lower concrete density [82]. The WA indices of the SER blend were 6%, 19%, and 23.33% more improved than those of the POT after curing periods of twenty-eight, ninety, and one hundred and twenty days. When the SUG was utilized for mixing, the WA increased by 10% after twenty-eight days, another 13% after ninety days, and 18% after 180 days [45].

3.2.2. Chloride Ion Migration

The diffusion of chloride ions into concrete is investigated in this study using 4 percent NaCl. The criterion for determining this feature is the depth in millimeters to which these chloride ions propagate inside the concrete matrix. The chloride ion migration values for all of the FRAC compositions are shown in Figure 8. The highest values for chloride ion movement were found in the FER, which was rich in chloride, iron, and sulfate ions. Coal ash decreases chloride ion migration by forming CSH gel and filling voids of paste, which is attributed to the dense matrix of the concrete.

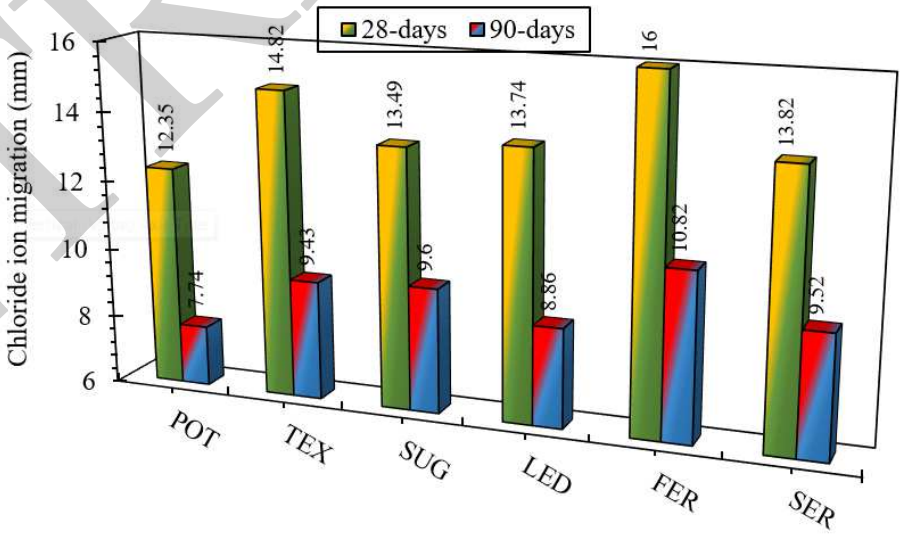


Figure 8. Chloride ion migration in all FRAC compositions at twenty-eight and ninety days of testing.

The reference mix (POT) revealed 12.3 mm and 7.7 mm of chloride ion mobility after twenty-eight days and ninety days, individually. After curing for ninety days, coal ash concrete representatives produced reduced results for the chloride ion migration, showing the effect of the pozzolanic process in ameliorating the long-term durability of concrete compositions with effluent. The representatives made with the POT presented the lowest chloride ion migration at twenty-eight as well as ninety days because of the production of

RETRACTED

both CSH gel and sulphoaluminate hydrate, which efficiently enhanced the cohesion of the ITZ coats. Similar conclusions were observed in previous investigations [22,83].

The TEX blend revealed chloride ion diffusion that was 16.5% and 18% more enhanced than that of the POT at twenty-eight and ninety days, respectively. It suggests that while using the TEX blend, the steel bars are more susceptible to rust and degradation. Through the oxidation process of iron available in the TEX mix, Cl^- performed as a catalyst to produce a $FeCl_3^-$ compound. This compound was unstable, and joined with OH^- to develop $Fe(OH)_2$. Finally, the Cl^- converted to free ions and returned to the mixture for the reaction with OH^-. The compound $Fe(OH)_2$ resulted in a reduced value of pH, which minimized the oxide film and allowed easier migration of chloride ions. The FER mix also demonstrated 16 mm and 10.8 mm of chloride ion migration at twenty-eight days and ninety days, respectively. The FER degrades concrete and enables chloride ions to diffuse more quickly since it is high in chloride and sulfate [84]. The relatively low pH of FER also enhances chloride ion migration [80].

The chloride ion mobility values in the LED were larger than those in the control mix because the LED included less iron. The SER mix revealed a chloride ion migration of 13.8 mm and 9.5 mm at twenty-eight and ninety days, respectively, which is 10.5% and 18% more improved than the POT values. The chloride ion mobility levels in the SUG mix were identical to those in the SER blend. As a consequence, SUG had the lowest chloride ion migration of all the effluent types investigated, which predicts that it is less prone to corrosion. The maximum chloride ion migration values were found in the FER, indicating that it is more prone to corrosion.

3.2.3. Resistance against H_2SO_4 Attack

The alkaline composition of concrete defines it as particularly susceptible to acid attack. When sewerage systems are under acid attack, the effluent infrastructure starts deteriorating. This is why acid attack protection has emerged as an important durability indicator to monitor. The most active and destructive of all the acids is H_2SO_4 due to its low pH. It rapidly reacts with CH to form $CaSO_4$ which is the primary cause of deterioration. This research showed the mass loss of representatives (as measured by concrete degradation) after immersion in a 4% H_2SO_4 solution for twenty-eight, ninety, and one hundred and twenty days. Figure 9 shows the mass loss observed by all other FRAC blends. The most notable reduction was in the FER mix. The inclusion of coal ash lowers the acid absorption of FRAC and causes the production of CSH gel. As a result, H_2SO_4 infiltration in FRAC will be lower, resulting in a reduced mass loss at various testing ages.

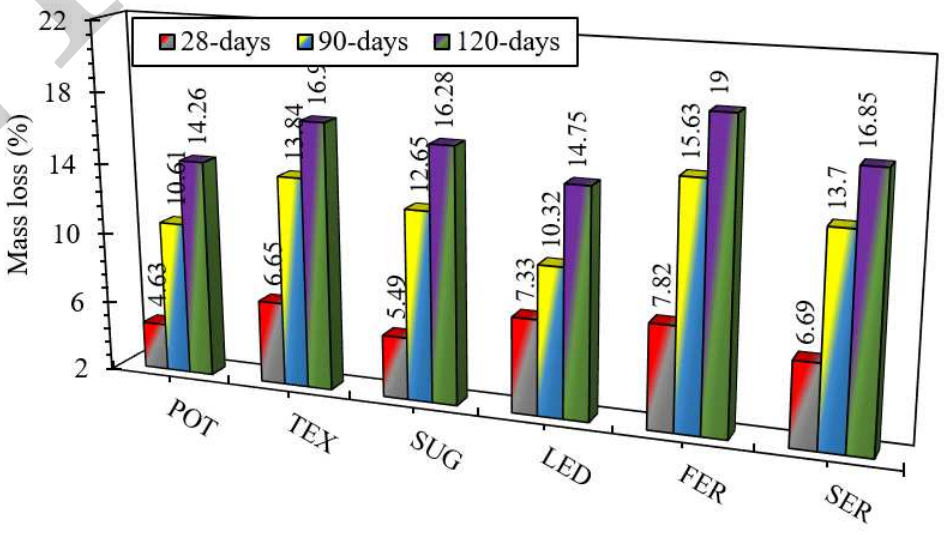


Figure 9. Mass loss of FRAC compositions due to the attack of H_2SO_4 at twenty-eight, ninety, and one hundred and twenty days.

RETRACTED

The TEX mixture degrades at a faster rate than the reference mix. The TEX had mass losses of 6.6%, 13.8%, and 16.9%, respectively, after a curing period of twenty-eight, ninety, and one hundred and twenty days, which was an average of 29.5%, 22.0%, and 17% more improved than the reference blend. The FER showed a mass reduction of 7.8%, 15.6%, and 19% after twenty-eight, ninety, and one hundred and twenty days, which were 40%, 32%, and 26% more improved than the reference mix. As the mass loss is increased, the pH value for the mixing water is decreased. As a result of having the lowest pH value, the FER mix may have the highest mass loss [47,48]. As a result, the pH of the acid, as well as the mixing effluent, have a significant impact on concrete degradation [85,86]. Moreover, the FER's high sulfate content may account for the increased mass loss. The LED mix degraded more quickly at first, but after ninety and one hundred and twenty days, the rate of deterioration was approximately comparable to that of the POT. At twenty-eight, ninety, and one hundred and twenty days, the SER blend showed mass reductions of 6.6%, 13.7%, and 16.8%, respectively, which were 29.5%, 23%, and 15% more improved than the POT mix. At twenty-eight, ninety, and one hundred and twenty days, the SUG mix showed mass reductions of 5.5%, 12.6%, and 16.3%, respectively, which were larger due to the H_2SO_4 attack. As a result, we may affirm that the effluent of all types studied in this research promotes concrete deterioration. Figure 10 shows the relative mass losses caused by the acid attacks on different concrete mixtures at various testing ages.

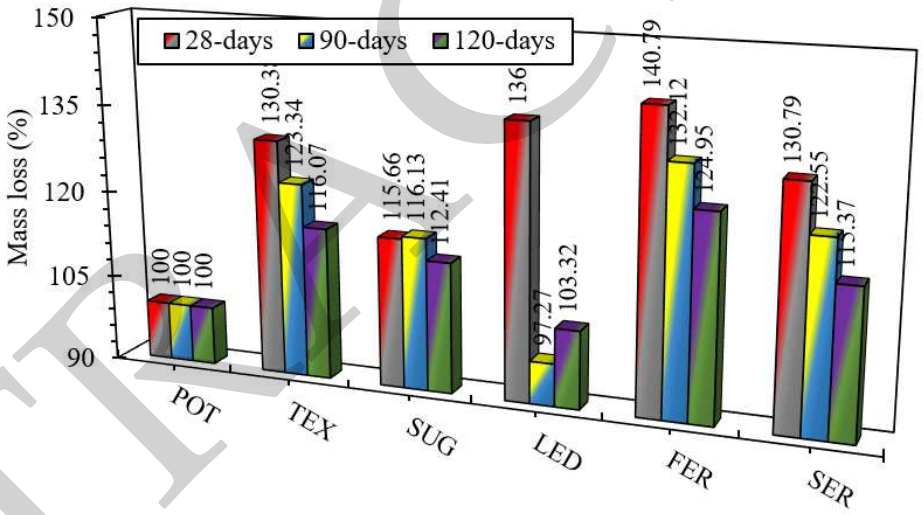


Figure 10. Mass loss of FRAC compositions with regards to POT at twenty-eight, ninety, and one hundred and twenty days.

3.3. Statistical Analysis

The ANOVA test was utilized to analyze the significance of deviations in various durability features of the FRAC blends at ninety days and mechanical parameters at twenty-eight days of the testing ages. The findings of the ANOVA analysis at a 5% statistical significance are shown in Tables 6–9. Three representatives were collected from each of the six groups (POT, TEX, FER, LED, SER, and SUG) in the FRAC blend. To effectively demonstrate the value of the experimental outcomes, a comparison was made between all of the FRAC blends and the reference mix (POT). With a *p*-value of more than 5% in a 95% confidence interval and a value of F smaller than F_{crit}, the ANOVA test indicates that the amount of variation in the three FRAC mixtures is minor. In this scenario, the ANOVA analysis findings at a notable threshold of 5% revealed that after twenty-eight days, the FRAC blends had a major difference (p = 0.02 percent and $F > F_{crit}$) in their CS, indicating that the effluent types tested had a substantial impact on the CS of FRAC. The STS (p = 27 percent and $F < F_{crit}$), WA test (p = 10 percent and $F < F_{crit}$), and sulphuric acid attack test (p = 20 percent and $F < F_{crit}$) results, on the other hand, did not demonstrate any significant differences among different FRAC compositions. The chloride ion migration

RETRACTED

findings of FRAC blends also showed a major difference with a probability of 0.04% and $F > F_{crit}$), indicating that the effluent types tested in FRAC mixing influenced the chloride ion migration outcomes.

Table 6. ANOVA test for the CS of FRAC compositions.

Groups	Count	Sum	Average	Variance			
POT	3	63.02774	21.00924667	2.219700211			
LED	3	42.714375	14.238125	7.903666312			
FER	3	58.973625	19.657875	4.303503563			
TEX	3	83.619	27.873	4.684854938			
SUG	3	61.652625	20.550875	3.827338922			
SER	3	66.21975	22.07325	4.772577937			
			ANOVA				
Source of variation	Sum of squares	Degrees of freedom	Mean squares		F	p-value	F_{crit}
Between groups	288.1695593	5	57.63391185		8.47863525	0.000206664	3.105875239
Within groups	55.42328377	12	4.61860698				
Total	343.592843	17					

Table 7. ANOVA test for the STS of FRAC compositions.

Groups	Count	Sum	Average	Variance			
POT	3	6.05625	2.01875	0.001032234			
LED	3	5.6715	1.8905	0.050376422			
FER	3	5.778375	1.926125	0.006819516			
TEX	3	7.103625	2.367875	0.176529			
SUG	3	5.835375	1.945125	0.052237828			
SER	3	5.735625	1.911875	0.118097766			
			ANOVA				
Source of variation	Sum of squares	Degrees of freedom	Mean squares		F	p-value	F_{crit}
Between groups	0.489910844	5	0.097982169		1.451255274	0.275778446	3.105875239
Within groups	0.810185531	12	0.067515461				
Total	1.300096375	17					

Table 8. ANOVA test for the chloride ion migration of FRAC compositions.

Groups	Count	Sum	Average	Variance			
POT	3	23.231985	7.743995	1.132812315			
LED	3	24.46437	8.15479	0.754597331			
FER	3	28.568925	9.522975	4.678102345			
TEX	3	28.283745	9.427915	4.715792447			
SUG	3	32.44941	10.81647	0.808297081			
SER	3	28.813365	9.604455	0.60030996			
			ANOVA				
Source of variation	Sum of squares	Degrees of freedom	Mean squares		F	p-value	F_{crit}
Between groups	18.43320295	5	3.68664059		1.743104637	0.199393883	3.105875239
Within groups	25.37982296	12	2.114985246				
Total	43.81302591	17					

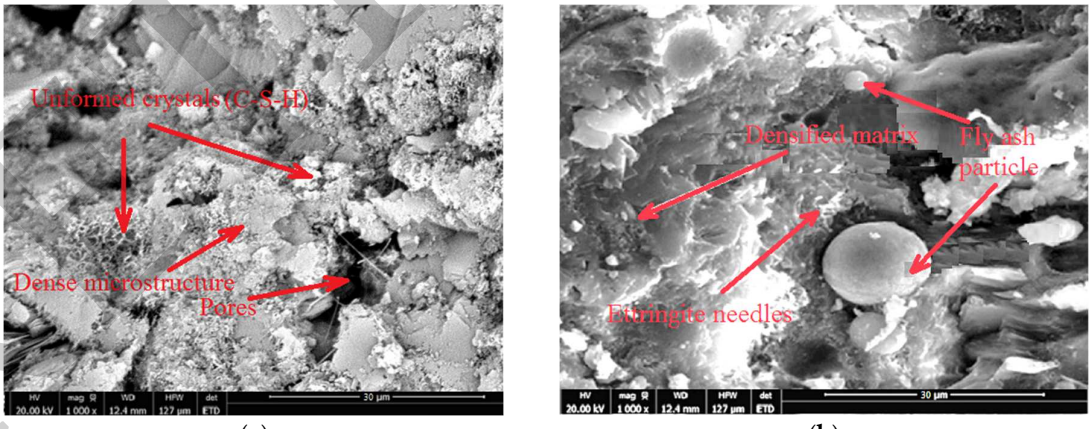
RETRACTED

Table 9. ANOVA test for the sulfuric acid attack of FRAC compositions.

Groups	Count	Sum	Average	Variance		
POT	3	31.8402252	10.6134084	0.604905146		
LED	3	30.9456084	10.3152028	2.151876247		
FER	3	41.1015423	13.7005141	1.005832652		
TEX	3	41.5183524	13.8394508	1.037664326		
SUG	3	46.8962193	15.6320731	1.098640583		
SER	3	37.9500513	12.6500171	0.888944267		
			ANOVA			
Source of variation	Sum of squares	Degrees of freedom	Mean squares	*F*	*p*-value	F_{crit}
Between groups	62.66853252	5	12.5337065	7.07892669	0.000364576	3.105875239
Within groups	13.57572644	12	1.131310537			
Total	76.24425896	17				

3.4. Scanning Electron Microscopic Analysis

SEM analysis was employed to examine the microstructure of the fabricated compositions. In the POT mix, CSH gel crystals, whose shape can be observed in Figure 11a, were produced. The crystals produced in the structure of concrete utilizing the POT were semi-shaped and unshaped, and their surface was mostly not detectible; though the concrete fabricated using various types of effluent produced a decent crystalline shape, and their numerous surfaces are identifiable. These unshaped crystals in the POT mix can be referred to as rocky soils having no well-formed crystalline surface. Moreover, the distance between the crystals in the concrete produced using effluent types was larger than that in the concrete mix produced using the POT. The POT mix showed the densified microstructure, due to which it presented better results than all types of effluent. This may be ascribed to the reduced CS of the representatives produced using effluent types [87]. Figure 11b shows the SEM image of concrete produced using fertilizer effluent (FER mix). The unreacted coal ash particles are also visible in the structure. A larger distance between the crystals which are well-shaped and organized can be seen in the microstructure of the FER mix. The crystals of CSH gel are sharp-edged, well-formed, and well-shaped, which can be easily detected from their surfaces.



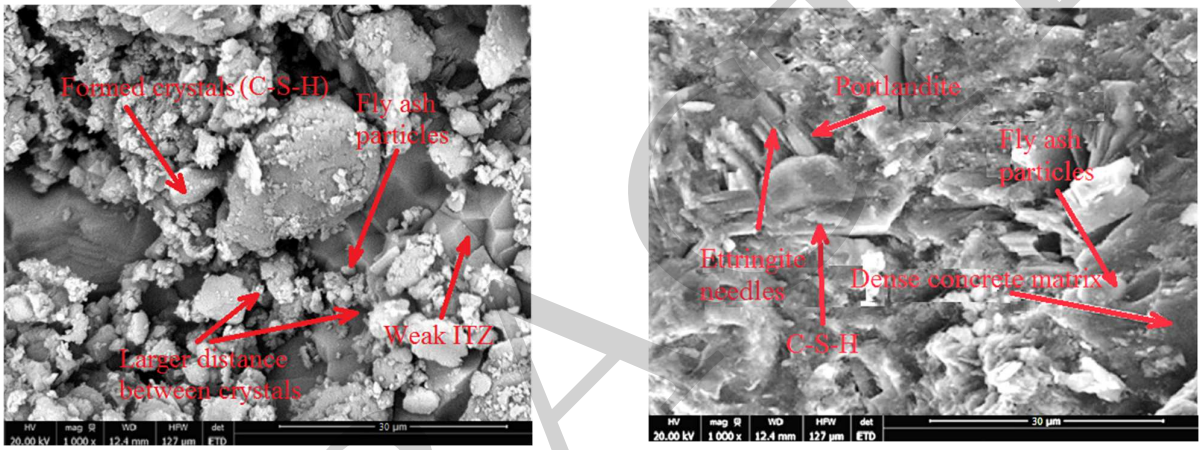
(**a**) (**b**)

Figure 11. SEM images of concrete compositions (**a**) POT mix (**b**) FER mix.

Figure 12a shows the microstructural analysis of the LED mix through an SEM image. The concrete mix consisting of leather industry effluent showed more voids in the structure compared to the other compositions. This resulted in the reduced CS of the mix. The presence of organic matter in LED water, which was spongy, produced an impact on the water demand, resulting in the reduced mechanical performance of the LED mix [67,68]. The SEM image of the TEX mix is presented in Figure 12b. The figure verified the presence

RETRACTED

of the CSH gels and ettringite needles in the structure. The coal ash particles were enclosed with some of the hydrated compounds. For all FRAC compositions with effluent, the pozzolanic chemical process of the coal ash particles was improved because of the various compounds in the effluent and coal ash attached to the microstructure of the compositions; consequently, the hydrated products were ameliorated. The ions are interchanged nearby between the CSH phase and other particles from the textile factory effluent. The *Ca* ions are diffused from the porous solution and substituted by *Mg*. Furthermore, the *Mg* ions diffused into the CSH gel. This phenomenon verifies that the chemical reaction occurred on the surface of coal ash particles, which produced silicate ions leading to the production of CSH gel in the ITZ [88–90]. Additionally, the strength of ITZ is improved due to the chemical reaction on the outer surface of the particles resulting in an ameliorated mechanical performance on the concrete mix [90–92]. The increased amounts of silicates that lead to improving the CS with smaller contents of cement improved the ITZ and enhanced the mechanical performance of the TEX mix.



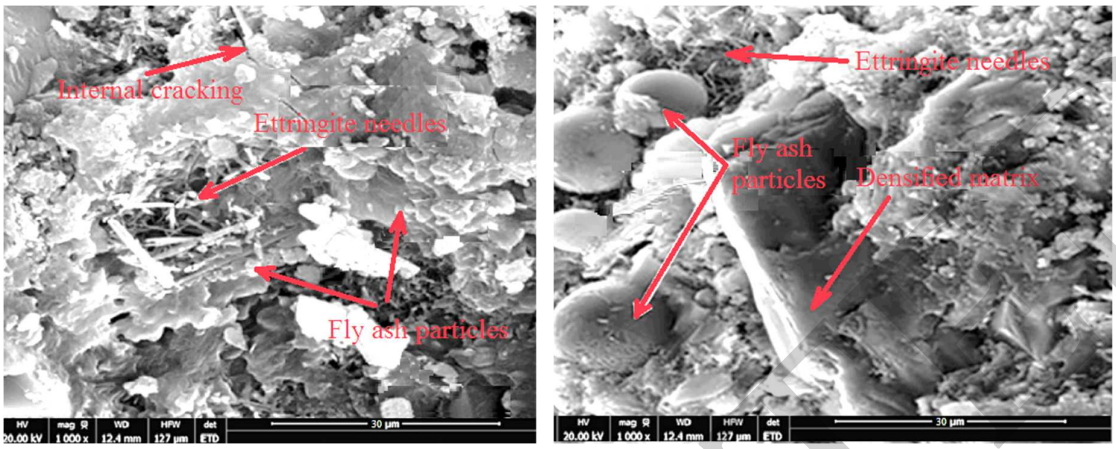
(**a**) (**b**)

Figure 12. SEM images of concrete compositions (**a**) LED mix (**b**) TEX mix.

Figure 13a presents the SEM analysis of the SUG mix while Figure 13b shows the SEM analysis of the SER mix. Both compositions produced substantial quantities of un-hydrated cement, porosity, and continuous internal cracking at different locations because of the sulfate, zinc, and TSS, which resulted in a hindrance of the cement hydration process and deteriorated the ITZ coat between the cement matrix and aggregates. This can also be ascribed to the TSS in concrete producing the lesser CS and durability performance of compositions with effluent compared with the POT mix [93]. Additionally, numerous weak ITZ layers are present between the cement matrix and RCA in SUG and SER compositions. These weak layers, finally, encouraged the internal cracking of concrete and increased porosity, resulting in a decrease in the adhesive stresses between the concrete matrix and RCA. Consequently, FRAC compositions produced lesser durability and mechanical behavior than the POT mix. Furthermore, the SEM results show that the SUG, TEX, FER, and SER compositions produced ettringite needles, resulting in a high quantity of *Ca* in RCA, which augmented the development of ettringite needles. Nevertheless, the ettringite needles were not presented in mix LED due to the *Ca* ions in RCA reacting with sulfate and producing *Ca*. monosulphoaluminate hydrate. This reveals why the SUG, TEX, FER, and SER compositions produced lesser porosity and chloride ion migration than mix LED. Additionally, all coal ash concrete compositions presented the most densified microstructure except the LED mix due to the CSH gel and the tiny-sized spherical particles of coal ash, which have efficiently occupied pores that were encouraged by the adhered mortar of RCA and the TSS, and therefore improved the weak ITZ layers [93]. Consequently, the recycled aggregate concrete mix produced with TEX effluent and coal ash particles

RETRACTED

presented considerably improved durability bavior as compared with the compositions fabricated using other types of effluent.



(**a**) (**b**)

Figure 13. SEM images of concrete compositions (**a**) SUG mix (**b**) SER mix.

4. Conclusions

The experimental findings resulted in the following main conclusions:

1. The CS of the FRAC blend fabricated using textile factory effluent at ninety days was maximum at a value of 30.5 MPa, which was 19% more improved than the CS of concrete manufactured with potable water. The inclusion of coal ash resulted in a pozzolanic interaction between CH and coal ash particles, which led to a surge in the CS of FRAC. Furthermore, the inclusion of coal ash into concrete surges the density of the matrix. A strong bond developed between cement and sand particles due to CSH gel.
2. At ninety days, the STS of concrete made with textile industry effluent was approximately 115 percent more improved than the STS of concrete made with potable water. When equated with concrete produced using potable water, the FRAC compositions made with fertilizer factory effluent had a maximum STS of 97 percent, the mix made with leather factory effluent had a maximum STS of 92 percent, the service station effluent FRAC mix had a maximum STS of 99 percent, and the sugar factory effluent FRAC mix had a maximum STS of 95 percent.
3. The test results revealed that, among all the different FRAC compositions, concrete made with leather factory effluent had the highest WA, i.e., 113 percent and 121 percent at twenty-eight and ninety days, separately. This depicts that concrete made using leather factory effluent has a lot of pores and less density, being less durable. The coal ash inclusion reduced the WA of FRAC compositions.
4. The maximum level of chloride ion migration showed by concrete manufactured utilizing fertilizer factory effluent, i.e., 16 mm at twenty-eight days and 10.8 mm at ninety days as compared to the control mix.
5. The results of tests in which FRAC compositions were exposed to a 4 percent solution of H_2SO_4 revealed that the FRAC mix made with fertilizer factory effluent lost mass due to acid attack, i.e., 19 percent after 120 days. This could be explained by the fact that the pH value of fertilizer factory effluent was the lowest (2.5), which enhanced the mass loss. Adding coal ash to FRAC compositions proved to be helpful for the development of the durability behavior of the concrete.
6. The ANOVA analysis revealed major variations between the CS and chloride ion migration results of different FRAC blends. On the other hand, FRAC mixtures exhibited no significant changes in STS, WA, or acid attack. Therefore, the investigated

RETRACTED

types of effluent can be utilized to make efficient concrete, which leads to waste material availability and long-term environmental impact.

7. The SEM results depicted that the mix TEX presented the most densified microstructure with the formation of CSH gels and ettringite needles, having an improved ITZ compared with the other types of effluent, thus leading to the enhanced mechanical and durability performance of the FRAC mix.

Author Contributions: Conceptualization, A.R. and A.B.E.; methodology, A.R. and M.A.; software, N.S., K.M.E., A.F.D., A.B.E. and K.A.; validation, M.A., A.F.D., A.B.E. and K.A.; formal analysis, M.A., A.F.D., A.B.E. and K.A.; investigation, A.R., N.S. and K.A.; resources, K.M.E., A.B.E. and K.A.; data curation, M.A., A.F.D., A.B.E. and K.A.; writing—original draft preparation, A.R. and K.A.; writing—review and editing, N.S., K.M.E., M.A., A.F.D., and A.B.E.; visualization, M.A., A.F.D., A.B.E. and K.A.; supervision, A.R., and K.A.; project administration, A.R. and A.B.E.; funding acquisition, M.A. and K.M.E. All authors have read and agreed to the published version of the manuscript.

Funding: This research was funded by the Deanship of Scientific Research at King Khalid University for funding this work through the Large Groups Project under grant number R.G.P. 2/152/43.

Data Availability Statement: All data have been presented in this work.

Acknowledgments: The Authors extend their appreciation to the Deanship of Scientific Research at King Khalid University for funding this work through the Large Groups Project under grant number R.G.P. 2/152/43.

Conflicts of Interest: The authors declare no competing interest.

References

1. McGinnis, M.J.; Davis, M.; De La Rosa, A.; Weldon, B.D.; Kurama, Y.C. Quantified sustainability of recycled concrete aggregates. *Mag. Concr. Res.* **2017**, *69*, 1203–1211. [CrossRef]
2. Coelho, A.; de Brito, J. Influence of construction and demolition waste management on the environmental impact of buildings. *Waste Manag.* **2012**, *32*, 532–541. [CrossRef]
3. Azúa, G.; González, M.; Arroyo, P.; Kurama, Y. Recycled coarse aggregates from precast plant and building demolitions: Environmental and economic modeling through stochastic simulations. *J. Clean. Prod.* **2018**, *210*, 1425–1434. [CrossRef]
4. Xiao, J.Z.; Wang, C.; Ding, T.; Akbarnezhad, A. A recycled aggregate concrete high-rise building: Structural performance and embodied carbon footprint. *J. Clean. Prod.* **2018**, *199*, 868–881. [CrossRef]
5. Silva, R.V.; Brito, J.D.; Dhir, R.K. Fresh-state performance of recycled aggregate con-crete: A review. *Constr. Build. Mater.* **2018**, *178*, 19–31. [CrossRef]
6. Ozbakkaloglu, T.; Gholampour, A. Time-dependent and long-term mechanical properties of concretesincorporating different grades of coarse recycled concrete aggregates. *Eng. Struct.* **2018**, *157*, 224–234.
7. Oh, D.-Y.; Noguchi, T.R.; Kitagaki, W.; Park, J. CO_2 emission reduction by reuse of building material waste in the Japanese cement industry. Renew. *Sustain. Energy Rev.* **2014**, *38*, 796–810. [CrossRef]
8. Kurad, R.; Silvestre, J.D.; de Brito, J.; Ahmed, H. Effect of incorporation of high volume of recycled concrete aggregates and fly ash on the strength and global warming potential of concrete. *J. Clean. Prod.* **2017**, *166*, 485–502. [CrossRef]
9. Tariq, H.; Siddique, R.M.A.; Shah, S.A.R.; Azab, M.; Rehman, A.U.; Qadeer, R.; Ullah, M.K.; Iqbal, F. Mechanical Performance of Polymeric ARGF-Based Fly Ash-Concrete Composites: A Study for Eco-Friendly Circular Economy Application. *Polymers* **2022**, *14*, 1774. [CrossRef]
10. Raza, A.; Shah, S.A.R.; Kazmi, S.N.H.; Ali, R.Q.; Akhtar, H.; Fakhar, S.; Khan, F.N.; Mahmood, A. Performance evaluation of concrete developed using various types of wastewater: A step towards sustainability. *Constr. Build. Mater.* **2020**, *262*, 120608. [CrossRef]
11. Raza, A.; Rafique, U. Efficiency of GFRP bars and hoops in recycled aggregate concrete columns: Experimental and numerical study. *Compos. Struct.* **2020**, *255*, 112986. [CrossRef]
12. More, A.B.; Ghodake, R.B.; Nimbalkar, H.N.; Chandake, P.P.; Maniyar, S.P.; Narute, Y.D. Reuse of treated domestic wastewater in concrete—A sustainable approach. *Indian J. Appl. Res.* **2014**, *4*, 182–184. [CrossRef]
13. Al-Jabri, K.; Al-Saidy, A.; Taha, R.; Al-Kemyani, A. Effect of using Wastewater on the Properties of High Strength Concrete. *Procedia Eng.* **2011**, *14*, 370–376. [CrossRef]
14. Ghafoor, S.; Hameed, A.; Shah, S.A.R.; Azab, M.; Faheem, H.; Nawaz, M.F.; Iqbal, F. Development of Construction Material Using Wastewater: An Application of Circular Economy for Mass Production of Bricks. *Materials* **2022**, *15*, 2256. [CrossRef]
15. Hassani, M.S.; Asadollahfardi, G.; Saghravani, S.F.; Jafari, S.; Peighambarzadeh, F.S. The difference in chloride ion diffusion coefficient of concrete made with drinking water and wastewater. *Constr. Build. Mater.* **2019**, *231*, 117182. [CrossRef]

REJECTED

16. Verian, K.P.; Ashraf, W.; Cao, Y. Properties of recycled concrete aggregate and their influence in new concrete production. *Resour. Conserv. Recycl.* **2018**, *133*, 30–49. [CrossRef]
17. Kisku, N.; Joshi, H.; Ansari, M.; Panda, S.; Nayak, S.; Dutta, S.C. A critical review and assessment for usage of recycled aggregate as sustainable construction material. *Constr. Build. Mater.* **2017**, *131*, 721–740. [CrossRef]
18. Xiao, J.; Li, W.; Fan, Y.; Huang, X. An overview of study on recycled aggregate concrete in China (1996–2011). *Constr. Build. Mater.* **2012**, *31*, 364–383. [CrossRef]
19. Contreras Llanes, M.; Romero Pérez, M.; Gázquez González, M.J.; Bolívar Raya, J.P. Construction and demolition waste as recycled aggregate for environmentally friendly concrete paving. *Environ. Sci. Pollut. Res.* **2021**, *29*, 1–15.
20. Kaplan, G.; Gulcan, A.; Cagdas, B.; Bayraktar, O.Y. The impact of recycled coarse aggregates obtained from waste concretes on lightweight pervious concrete properties. *Environ. Sci. Pollut. Res.* **2021**, *28*, 17369–17394. [CrossRef]
21. Ali, B.; Fahad, M.; Mohammed, A.S.; Ahmed, H.; Elhag, A.B.; Azab, M. Improving the performance of recycled aggregate concrete using nylon waste fibers. *Case Stud. Constr. Mater.* **2022**, *17*, e01468. [CrossRef]
22. Ali, B.; Qureshi, L.A.; Shah, S.H.A.; Rehman, S.U.; Hussain, I.; Iqbal, M. A step towards durable, ductile and sustainable concrete: Simultaneous incorporation of recycled aggregates, glass fiber and fly ash. *Constr. Build. Mater.* **2020**, *251*, 118980. [CrossRef]
23. Sivamani, J.; Renganathan, N.T. Effect of fine recycled aggregate on the strength and durability properties of concrete modified through two-stage mixing approach. *Environ. Sci. Pollut. Res.* **2021**, 1–14. [CrossRef] [PubMed]
24. Yang, F.; Yao, Y.; Wang, X.; Wei, J.; Feng, Z. Preparation of recycled and multi-recycled coarse aggregates concrete with the vibration mixing process. *Buildings* **2022**, *12*, 1369. [CrossRef]
25. McNeil, K.; Kang, T.H.-K. Recycled concrete aggregates: A review. *Int. J. Concr. Struct. Mater.* **2013**, *7*, 61–69. [CrossRef]
26. Rahal, K. Mechanical properties of concrete with recycled coarse aggregate. *Build. Environ.* **2007**, *42*, 407–415. [CrossRef]
27. Dabhade, A.; Choudhari, S.; Gajbhiye, A. Performance evaluation of recycled aggregate used in concrete. *Int. J. Eng. Res. Appl.* **2012**, *2*, 1387–1391.
28. López-Uceda, A.; Galvín, A.P.; Barbudo, A.; Ayuso, J. Long-term leaching and mechanical behaviour at recycled aggregate with different gypsum contents. *Environ. Sci. Pollut. Res.* **2019**, *26*, 35565–35573. [CrossRef]
29. Etxeberria, M.; Vázquez, E.; Mari, A.; Barra, M. Influence of amount of recycled coarse aggregates and production process on properties of recycled aggregate concrete. *Cem. Concr. Res.* **2007**, *37*, 735–742. [CrossRef]
30. Mukharjee, B.B.; Barai, S.V. Influence of Nano-Silica on the properties of recycled aggregate concrete. *Constr. Build. Mater.* **2014**, *55*, 29–37. [CrossRef]
31. Li, W.; Xiao, J.; Sun, Z.; Kawashima, S.; Shah, S.P. Interfacial transition zones in recycled aggregate concrete with different mixing approaches. *Constr. Build. Mater.* **2012**, *35*, 1045–1055. [CrossRef]
32. Huda, S.B.; Shahria Alam, M. Mechanical and freeze-thaw durability properties of recycled aggregate concrete made with Recycled coarse aggregate. *J. Mater. Civ. Eng.* **2015**, *27*, 04015003. [CrossRef]
33. Duan, Z.; Poon, C.S. Properties of recycled aggregate concrete made with recycled aggregates with different amounts of old adhered mortars. *Mater. Des.* **2014**, *58*, 19–29. [CrossRef]
34. Wang, X.; Yan, Y.; Tong, X.; Gong, Y. Investigation of mineral admixtures on mechanical properties of alkali-activated recycled concrete Powders Cement. *Buildings* **2022**, *12*, 1234. [CrossRef]
35. Bílek, V. Development of alkali-activated concrete containing recycled wash water. In Proceedings of the 2nd Int. Conf. Sustain. Constr. Mater. Technologies, Ancona, Italy, 28 June 2010; pp. 309–318.
36. Cebeci, O.Z.; Saatci, A.M. Domestic sewage as mixing water in concrete. *ACI Mater. Jour.* **1989**, *86*, 503–506.
37. Sandrolini, W.; Franzoni, E. Waste wash water recycling in ready mixed concrete plants. *Cem. Concr. Res.* **2001**, *31*, 485–489. [CrossRef]
38. Lee, O.S.S.; Salim, M.R.; Ismail, M.R.; Ali, M.I. Reusing treated effluent in concrete technology. *Jour. Tech.* **2001**, *34*, 1–10.
39. Ghusain, A.I.; Terro, M.J. Use of treated wastewater for concrete mixing in Kuwait. *Kuw. Jour. Sci. Eng.* **2003**, *30*, 213–228.
40. Shekarchi, M.; Yazdian, M.; Mehrdadi, N. Use of biologically treated domestic wastewater in concrete. *Kuw. Jour. Sci. Eng.* **2009**, *39*, 97–111.
41. Asadollahfardi, G.; Asadi, M.; Jafari, H.; Moradi, A.; Asadollahfardi, R. Experimental and statistical studies of using wash water from ready-mix concrete trucks and a batching plant in the production of fresh concrete. *Constr. Build. Mater.* **2015**, *98*, 305–314. [CrossRef]
42. Yao, X.; Xu, Z.; Guan, J.; Liu, L.; Shangguan, L.; Xi, J. Influence of wastewater content on mechanical properties, microstructure, and durability of concrete. *Buildings* **2022**, *12*, 1343. [CrossRef]
43. Asadollahfardi, G.; Tahmasabi, G.; Nabi, S.M.; Pouresfandyani, H.; Hossieni, S.A.A. Effects of using concrete wash water on a few characteristics of new concrete. *Environ. Eng. Manag. J.* **2017**, *16*, 1569–1575. [CrossRef]
44. Wasserman, B. Wash Water in the Mix: Effects on the Compressive Strength of Concrete. *Int. J. Constr. Educ. Res.* **2012**, *8*, 301–316. [CrossRef]
45. Saxena, S.; Tembhurkar, A.R. Developing biotechnological technique for reuse of wastewater and steel slag in bio-concrete. *J. Clean. Prod.* **2019**, *229*, 193–202. [CrossRef]
46. Bahraman, M.; Asadollahfardi, G.; Salehi, A.M.; Yahyaei, B. Feasibility study of using wash water from ready mixed concrete plant and synthetic wastewater based on tap water with different total dissolved solid to produce self-compacting concrete. *J. Build. Eng.* **2021**, *41*, 102781. [CrossRef]

RETRACTED

47. De Belie, N.; Verselder, H.J.; De Blaere, B.; Van Nieuwenburg, D.; Verschoore, R. Influence of the cement type on the resistance of concrete to feed acids. *Cem. Concr. Res.* **1996**, *26*, 1717–1725. [CrossRef]
48. Pavlík, V.; Unčík, S. The rate of corrosion of hardened cement pastes and mortars with additive of silica fume in acids. *Cem. Concr. Res.* **1997**, *27*, 1731–1745. [CrossRef]
49. Varshney, H.; Khan, R.A.; Khan, I.K. Sustainable use of different wastewater in concrete construction: A review. *J. Build. Eng.* **2021**, *41*, 102411. [CrossRef]
50. *ASTM-C150/C150M-18*; Standard Specification for Portland Cement. ASTM International: West Conshohocken, PA, USA, 2018.
51. *ASTMC33/C33M-18*; Standard Specification for Concrete Aggregates. ASTM International: West Conshohocken, PA, USA, 2018.
52. *ASTM-C187*; Standard Test Method for the Determination of the Normal Consistency of the hydraulic Cement. ASTM International: West Conshohocken, PA, USA, 2017.
53. *ASTM-C115*; Standard Test Method for Fineness of Portland Cement by the Turbidimeter. ASTM International: West Conshohocken, PA, USA, 2010.
54. *ASTM-C151/C151M*; Standard Test Method for Autoclave Expansion of Hydraulic Cement. ASTM International: West Conshohocken, PA, USA, 2018.
55. *ASTM-C188*; Standard Test Method for Density of Hydraulic Cement. ASTM International: West Conshohocken, PA, USA, 2017.
56. *ASTM-C191*; Standard Test Methods for Time of Setting of Hydraulic Cement by Vicat Needle, ASTM C 191. ASTM International:: West Conshohocken, PA, USA, 2013.
57. *ASTM-C109*; Standard Test Method for Compressive Strength of Hydraulic Cement Mortars (Using 2-in. or [50-mm] Cube Specimens. ASTM International: West Conshohocken, PA, USA, 2016.
58. González, J.G.; Robles, D.R.; Valdés, A.J.; del Pozo, J.M.M.; Romero, M.I.G. Influence of moisture states of recycled coarse aggregates on the slump test. *Adv. Mater. Res.* **2013**, *742*, 379–383. [CrossRef]
59. *ASTM/C143*; Standard Test Method for Slump of Hydraulic Cement Concrete. ASTM International: West Conshohocken, PA, USA, 2005.
60. *C39/C39M-18, A.*; Standard Test Method for Compressive Strength of Cylindrical Concrete Specimens. ASTM International: West Conshohocken, PA, USA, 2018.
61. *C496M-17, A.C.*; Standard Test Method for Splitting Tensile Strength of Cylindrical Concrete Specimens. ASTM International: West Conshohocken, PA, USA, 2017.
62. *C1585-13, A.*; Standard Test Method for Measurement of Rate of Absorption of Water by Hydraulic-Cement Concretes. ASTM International: West Conshohocken, PA, USA, 2013.
63. Ali, B.; Qureshi, L.A. Influence of glass fibers on mechanical and durability performance of concrete with recycled aggregates. *Constr. Build. Mater.* **2019**, *228*, 116783. [CrossRef]
64. Abushanab, A.; Alnahhal, W. Combined effects of treated domestic wastewater, fly ash, and calcium nitrite toward concrete sustainability. *J. Build. Eng.* **2021**, *44*, 103240. [CrossRef]
65. Raza, A.; Rafique, U.; Haq, F.U. Mechanical and durability behavior of recycled aggregate concrete made with different kinds of wastewater. *J. Build. Eng.* **2020**, *34*, 101950. [CrossRef]
66. Mehrdadi, N.; Akbarian, A.; Haghollahi, A. Using domestic treated wastewater for producing and curing concrete. *J. Environ. Studues* **2009**, *35*, 129–136.
67. Naamane, S.; Rais, Z.; Taleb, M. The effectiveness of the incineration of sewage sludge on the evolution of physicochemical and mechanical properties of Portland cement. *Constr. Build. Mater.* **2016**, *112*, 783–789. [CrossRef]
68. Monzó, J.; Payá, J.; Borrachero, M.; Girbés, I. Reuse of sewage sludge ashes (SSA) in cement mixtures: The effect of SSA on the workability of cement mortars. *Waste Manag.* **2003**, *23*, 373–381. [CrossRef]
69. Tan, H.; Zou, F.; Liu, M.; Ma, B.; Guo, Y.; Jian, S. Effect of the adsorbing behavior of phosphate retarders on hydration of cement paste. *J. Mater. Civ. Eng.* **2017**, *29*, 04017088. [CrossRef]
70. Siler, P.; Kolarova, I.; Bednarek, J.; Janca, M.; Masilko, J.; Novotny, R.; Opravil, T. The effect of zinc, water to binder ratio and silica fume on the hydration and mechanical properties of Portland cement mixtures. *IOP Conf. Ser. Mater. Sci. Eng.* **2019**, *583*, 012008. [CrossRef]
71. Arooj, M.F.; Haseeb, F.; Butt, A.I.; Irfan-Ul-Hassan, M.; Batool, H.; Kibriya, S.; Javed, Z.; Nawaz, H.; Asif, S. A sustainable approach to reuse of treated domestic wastewater in construction incorporating admixtures. *J. Build. Eng.* **2020**, *33*, 101616. [CrossRef]
72. Gao, X.; Yang, Y.; Deng, H. Utilization of beet molasses as a grinding aid in blended cements. *Constr. Build. Mater.* **2011**, *25*, 3782–3789. [CrossRef]
73. Meena, K.; Luhar, S. Effect of wastewater on properties of concrete. *J. Build. Eng.* **2018**, *21*, 106–112. [CrossRef]
74. Akar, C.; Canbaz, M. Effect of molasses as an admixture on concrete durability. *J. Clean. Prod.* **2016**, *112*, 2374–2380. [CrossRef]
75. Ali, B.; Qureshi, L.A. Durability of recycled aggregate concrete modified with sugarcane molasses. *Constr. Build. Mater.* **2019**, *229*, 116913. [CrossRef]
76. Li, P.; Sui, L.; Xing, F.; Zhou, Y. Static and cyclic response of low-strength recycled aggregate concrete strengthened using fiber-reinforced polymer. *Compos. Part B Eng.* **2018**, *160*, 37–49. [CrossRef]
77. Venkateswara, R.V.S.R.; Jayaveera, K.N. *Effects of Alkalinity Present In Water on Strength and Setting Properties of Fly Ash Concrete*; CI-Premier PTE Ltd.: Orchard, Singapore, 2004.

RETRACTED

78. Mahasneh, B.Z. Assessment of Replacing Wastewater and treated water with Tap water in making Concrete Mix. *Electron. J. Geotech. Eng.* **2014**, *19*, 2379–2386. [CrossRef]
79. Reddy, V.V.; Ramana, N.V.; Gnaneswar, K.; Sashidhar, C. Effect of magnesium chloride (MgCl2) on ordinary Portland cement concrete. *Indian J. Sci. Technol.* **2011**, *4*, 643–645. [CrossRef]
80. Kucche, K.J.; Jamkar, S.S.; Sadgir, P.A. Quality of water for making concrete: A review of literature. *Int. J. Sci. Res. Publ.* **2015**, *5*, 1–10.
81. Asadollahfardi, G.; Delnavaz, M.; Rashnoiee, V.; Ghonabadi, N. Use of treated domestic wastewater before chlorination to produce and cure concrete. *Constr. Build. Mater.* **2016**, *105*, 253–261. [CrossRef]
82. SeyyedAlipour, S.F.; Kebria, D.Y.; Dehestani, M. Effects of recycled paperboard mill wastes on the properties of non-load-bearing concrete. *Int. J. Environ. Sci. Technol.* **2015**, *12*, 3627–3634. [CrossRef]
83. Ahmed, S.; Alhoubi, Y.; Elmesalami, N.; Yehia, S.; Abed, F. Effect of recycled aggregates and treated wastewater on concrete subjected to different exposure conditions. *Constr. Build. Mater.* **2020**, *266*, 120930. [CrossRef]
84. Sulikowski, J.; Kozubal, J. The durability of a concrete sewer pipeline under deterioration by sulphate and chloride corrosion. *Procedia Eng.* **2016**, *153*, 698–705. [CrossRef]
85. O'Connell, M.; McNally, C.; Richardson, M.G. Performance of concrete incorporating GGBS in aggressive wastewater environments. *Constr. Build. Mater.* **2012**, *27*, 368–374. [CrossRef]
86. Li, H.; Liu, J.; Chu, F.; Zhang, L. Study on mix proportion design based on strength and sulfate resistance of 100% recycled aggregate concrete. *Buildings* **2022**, *12*, 1467. [CrossRef]
87. Asadollahfardi, G.; Mahdavi, A.R. The feasibility of using treated industrial wastewater to produce concrete. *Struct. Concr.* **2018**, *20*, 123–132. [CrossRef]
88. Laibao, L.; Yunsheng, Z.; Wenhua, Z.; Zhiyong, L.; Lihua, Z. Investigating the influence of basalt as mineral admixture on hydration and microstructure formation mechanism of cement. *Constr. Build. Mater.* **2013**, *48*, 434–440. [CrossRef]
89. Sharaky, I.A.; Elamary, A.S.; Alharthi, Y.M. Effect of waste basalt fines and recycled concrete components on mechanical, water absorption, and microstructure characteristics of concrete. *Materials* **2022**, *15*, 4385. [CrossRef]
90. Tasong, W.; Cripps, J.; Lynsdale, C. Aggregate-cement chemical interactions. *Cem. Concr. Res.* **1998**, *28*, 1037–1048. [CrossRef]
91. Zhang, L.; Zhang, Y.; Liu, C.; Liu, L.; Tang, K. Study on microstructure and bond strength of interfacial transition zone between cement paste and high-performance lightweight aggregates prepared from ferrochromium slag. *Constr. Build. Mater.* **2017**, *142*, 31–41. [CrossRef]
92. Kuroda, M.; Watanabe, T.; Terashi, N. Increase of bond strength at interfacial transition zone by the use of fly ash. *Cem. Concr. Res.* **2000**, *30*, 253–258. [CrossRef]
93. Abushanab, A.; Alnahhal, W. Performance of sustainable concrete incorporating treated domestic wastewater, RCA, and fly ash. *Constr. Build. Mater.* **2022**, *329*, 127118. [CrossRef]

RETRACTED